ORTHODONTICS & CRANIOFACIAL RESEARCH

ORIGINAL ARTICLE

DOI: 10.1111/j.1601-6343.2011.01513.x

Morphological evaluation of cranial and maxillary shape differences of the brachymorphic mouse with spontaneous malocclusion using three-dimensional micro-computed tomography

F Saito
TS Kajii
Y Sugawara-Kato
Y Tsukamoto
Y Arai
Y Hirabayashi
O Fujimori
J Iida

Authors' affiliation:
F. Saito, T.S. Kajii, Y. Sugawara-Kato, Y. Tsukamoto, J. Iida, Department of Orthodontics, Division of Oral Functional Science, Graduate School of Dental Medicine, Hokkaido University, Sapporo, Japan
Y. Arai, School of Dentistry, Nihon University, Tokyo, Japan
Y. Hirabayashi, Laboratory of Anatomy and Physiology, Department of Health and Nutrition, School of Health and Human Life, Nagoya Bunri University, Inazawa, Aichi, Japan
O. Fujimori, Laboratory of Anatomy and Histochemistry, Department of Rehabilitation Science, Faculty of Human Health, Nagoya Gakuin University, Seto, Aichi, Japan

Correspondence to:
Takashi S. Kajii
Department of Orthodontics
Division of Oral Functional Science
Graduate School of Dental Medicine
Hokkaido University
Kita 13
Nishi 7
Kita-ku
Sapporo 060-8586
Japan
E-mail: kajii@den.hokudai.ac.jp

Dates:
Accepted 12 February 2011

To cite this article:
Saito F, Kajii TS, Sugawara-Kato Y, Tsukamoto Y, Arai Y, Hirabayashi Y, Fujimori O, Iida J: Morphological evaluation of cranial and maxillary shape differences of the brachymorphic mouse with spontaneous malocclusion using three-dimensional micro-computed tomography
Orthod Craniofac Res 2011;**14**:100–106

Structured Abstract

Authors – Saito F, Kajii TS, Sugawara-Kato Y, Tsukamoto Y, Arai Y, Hirabayashi Y, Fujimori O, Iida J

Objectives – The aim of this study was to determine whether significant cranial and maxillary deformity exists in BALB/c-*bm/bm* (brachymorphism) mouse with spontaneous malocclusion using three-dimensional (3D) images.

Materials and Methods – Thirty female mice were divided into the following three groups: control group (BALB/c mice, n = 10), Norm group (BALB/c-*bm/bm* mice with normal occlusion, n = 10), and Mal group (BALB/c-*bm/bm* mice with malocclusion, n = 10). Nine points in the skull were selected, and transverse and antero-posterior distances were measured using three-dimensional images of micro-computed tomography (CT). Moreover, 3D images were superimposed at the median plane to visualize the skull shape asymmetry.

Results – The transverse distances at the posterior cranial and maxillary region and the antero-posterior distances in the Norm and Mal groups were significantly shorter than those in the control group. The nasal septum of the Mal group was significantly shorter than that of the Norm group. Morphological measurements and superimposed 3D images showed that lateral deviation occurred at the anterior cranial and maxillary region in the Mal group.

Conclusion – The 3D micro-CT images revealed that the antero-posterior length and posterior transverse width at the cranium and maxilla in BALB/c-*bm/bm* mice were significantly smaller than those in BALB/c mice. It was quantitatively and morphologically clear that BALB/c-*bm/bm* mice show a spontaneous transverse crossbite owing to lateral deviation of the maxilla and nasal bone.

Key words: animal model; malocclusion; micro-CT; morphological measurement

Introduction

BALB/c-*bm/bm* mice (1) have a brachymorphic (*bm*) gene (2, 3) and various characteristics including a dome-shaped skull, short thick tail, and shortened but not widened limbs (4, 5). The most remarkable feature in the craniofacial region is a spontaneous malocclusion (incisal transverse crossbite) (5). Malocclusion occurs in about 10% of BALB/c-*bm/bm* mice

(5). Malocclusion does not spontaneously occur in mice with the same *bm* mutation as that in C57BL-*bm/bm* mice and in non-brachymorphic mice such as BALB/c-+/+ mice and BALB/c-*bm*/+ (*bm* heterozygotes) mice.

In human and murine tissues, all sulfation reactions are mediated through the universal sulfate donor 3′-phosphoadenosine 5′-phosphosulfate (PAPS) (6), and two different genes encoding the isoforms PAPS synthase (PAPSS) 1 and PAPSS2 have been identified (7). In the mouse, a missense mutation in the *Papss2* gene causes brachymorphism. The *Papss2* gene located on mouse chromosome 19 (6–9) is an autosomal recessive mutant gene. A disorder of PAPSS2 induces undersulfated glycosaminoglycans (GAGs) in the cartilage matrix and undersulfated GAGs lead to defective endochondral growth.

It was reported that columns of chondrocytes of BALB/c-*bm/bm* mice were irregularly arranged histologically and that undersulphated GAGs of the spheno-occipital synchondrosis and intersphenoid synchondrosis might cause disturbed of endochondral growth at the cranial base (5). There were no significant differences in the concentrations of sulphated GAGs in condyles between mandibular shifted and non-shifted sides in BALB/c-*bm/bm* mice with spontaneous malocclusion (10).

In BALB/c-*bm/bm* mice, lateral deviation between the maxillary and mandibular alveoli (i.e., malocclusion) has sometimes already occurred at birth (before the upper and lower incisors start to erupt). After the incisors erupt, the malocclusion becomes more apparent. In the mice that had malocclusion, the degree of lateral deviation of maxillary and mandibular alveoli and incisor was milder if incisors were cut after malocclusion occurred (11). This showed that premature contact between the upper and lower incisors continuously induced occlusal force on the maxillary and mandibular alveoli and the load aggravated the malocclusion in the animal model. From this finding, it is suggested that early intervention to reduce occlusal interference that promotes malocclusion could minimize malocclusion in growing orthodontic patients.

In the experiment (11) using two-dimensional headfilms, maxillary transverse deviation was found to be larger than mandibular deviation in BALB/c-*bm/bm* mice with malocclusion. However, no detailed information is available regarding the difference and the site. Studies using computed tomography (CT) have increased in recent years (12–18). The objective of the present study was to precisely determine whether significant cranial and maxillary hypo-growth and transverse deviations in BALB/c-*bm/bm* mice exist using three-dimensional (3D) morphological reconstructive images.

Materials and methods

Animals

Thirty adolescent female mice, aged 13 weeks, were divided into the following three groups: (1) BALB/c-+/+ mice (control group, n = 10), (2) BALB/c-*bm/bm* mice with normal occlusion (Norm group, n = 10), and (3) BALB/c-*bm/bm* mice with malocclusion (Mal group, n = 10). In the Mal group, five upper incisors were shifted to the right and five upper incisors were shifted to the left. BALB/c-+/+ mice (control mice) were obtained from Nippon Clea (Tokyo, Japan). By outbreeding between *bm* mice of the C57BL strain and normal mice of the BALB/c strain, the *bm* gene was successfully transferred to BALB/c strain mice (BALB/c-*bm*/+ mice) (11). BALB/c-*bm/bm* mice were generated by crossbreeding between BALB/c-*bm*/+ mice. In this paper, BALB/c-*bm/bm* mice are abbreviated as *bm/bm* mice. Dry skulls of each group were conventionally prepared by the standard protease method (19).

Morphological measurement

Images of dry skulls were obtained using 3D micro-CT (20) (R_mCT; Rigaku, Tokyo, Japan) under the following conditions: tube voltage, 90 kV; tube current, 120 μA; and slice width, 0.4 mm. Obtained CT images were morphologically reconstructed using image reconstruction software (i-VIEW-R; Morita, Kyoto, Japan).

Nine points were selected (Table 1). Among them, Oc, Tb, S2, and S1 were on both sides, while Ba, SC, N, Pr, and A were approximately on the median plane (Fig. 1A–C). We defined the anterior region as being in front of S1, the central region as being between S1 and S2, and the posterior region as being behind S2. In this study, the median plane was considered to be

***Table 1.* Definitions of the landmarks on cranium and maxilla**

Landmarks	Definitions
Oc	Most lateral points of the foramen magnum, located on the inner surface of the occipital bone
Tb	Posterior apex of the tympanic bulla
S2	Most posterior point on the zygomatic process of the temporal bone, at the intersection with the squamous part of the temporal bone
S1	Frontal point in the inner margin of the zygomatic arch
Ba	The frontal edge of the foramen magnum
SC	Point of intersection of the sagittal and the coronal sutures. In anatomy, this landmark is usually called Bregma
N	Medial point on frontonasal suture. In anatomy, this landmark is usually called Nasion
Pr	Most anterior point of the alveolar process in the incisive bone
A	Most anterior point of the nasal bone

perpendicular to a line that connected both S1 points, and at the same time, the plane passed through a point of N (frontonasal suture) (Fig. 1D), because various combinations of reference points were tested and this plane using the points of S1 and N was the closest to other median points (Ba, SC, N, Pr, A) in the control and Norm groups. The transverse distances from the median plane to Oc, Tb, S2, and S1 and the transverse deviations from the median plane to Ba, SC, Pr, and A were measured, and the antero-posterior (a-p) distances of Ba-SC, Ba-N, Ba-Pr, Ba-A, SC-N, SC-Pr, SC-A, N-Pr, N-A, and Pr-A were also measured. Using iVIEW-R, 3D coordinates (X, Y, Z) of all points were determined, and the linear distances between two points were calculated. The left side was measured in the control and Norm groups (21), and both the shifted and non-shifted sides were measured in the Mal group. The distances in the three groups were compared. Furthermore, the distances in the Mal group were

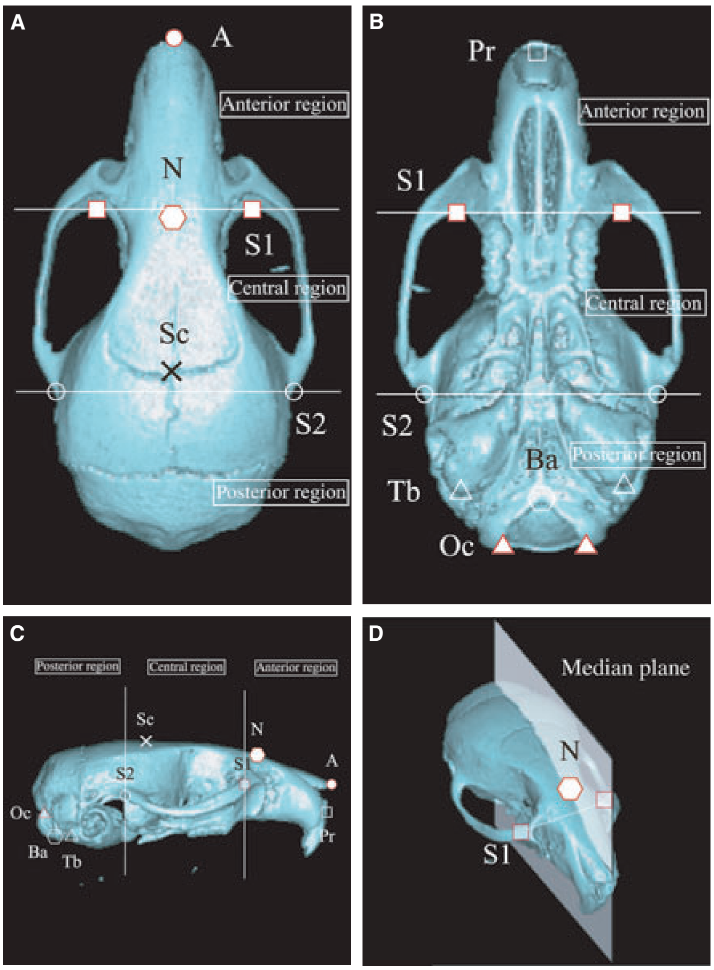

Fig. 1. Dorsal (A) and ventral (B) views. The lateral view (C) is shown to clarify the difference between points A and Pr. Oblique view (D) is helpful to understand the median plane.

compared between the shifted and non-shifted sides in the same regions.

Mirroring image

Original and reversal images of a mouse in the Mal group obtained using image reconstruction software were superimposed at the median plane using Adobe Photoshop CS version 10.0 (Adobe Systems, San Jose, CA, USA) to visualize the skull shape asymmetry.

The procedures were reviewed and approved by the animal care and use committees of Nagoya Bunri University and Hokkaido University, and this study was performed according to the Guidelines for Animal Experiments of Hokkaido University.

Statistical analysis

To assess measurement error, the same distance was measured on two different occasions with a time interval of 2 weeks by the same investigator (FS). There was a significant correlation between the first and second measurements of all distances in 30 mice ($p < 0.001$).

Statistically significant differences in measurement values among the three groups were evaluated using the Statistical Package for Social Science version 13.0 (SPSS Inc., Chicago, IL, USA) by one-way analysis of variance (ANOVA) with a probability level of $p < 0.05$ considered statistically significant. Tukey's HSD (honestly significant difference) test was used as the *post hoc* test.

Table 2. **Mean and standard deviation (SD) of each distance. Upper, transverse distances; middle, antero-posterior (a-p) distances; lower, transverse deviations**

Transverse distances	Control		Norm		Mal (non-shifted)		Mal (shifted)	
	Mean	SD	Mean	SD	Mean	SD	Mean	SD
Oc	2.50	0.41	1.94	0.19	1.79	0.39	2.17	0.31
Tb	3.91	0.27	3.35	0.26	3.29	0.38	3.48	0.29
S2	5.39	0.16	5.45	0.16	5.27	0.29	5.48	0.18
S1	3.80	0.15	3.63	0.19	3.51	0.30	3.72	0.22

a-p distances	Control		Norm		Mal	
	Mean	SD	Mean	SD	Mean	SD
Ba-SC	9.36	0.23	8.79	0.31	8.72	0.57
Ba-N	14.45	0.50	11.85	0.31	11.53	0.60
Ba-Pr	19.43	0.45	15.55	0.41	15.21	0.76
Ba-A	20.59	0.46	16.50	0.48	15.89	0.85
SC-N	7.23	0.36	6.40	0.38	6.07	0.55
SC-A	14.95	0.22	13.19	0.53	12.36	0.85
SC-Pr	15.31	0.22	14.06	0.53	13.44	0.58
N-Pr	8.83	0.25	8.29	0.31	7.91	0.31
N-A	7.83	0.27	6.87	0.29	6.41	0.39
Pr-A	3.35	0.27	3.20	0.17	3.01	0.26

Transverse deviations	Control		Norm		Mal	
	Mean	SD	Mean	SD	Mean	SD
Ba	0.34	0.33	0.18	0.17	0.25	0.22
SC	0.23	0.22	0.10	0.09	0.27	0.24
Pr	0.12	0.12	0.21	0.24	0.62	0.38
A	0.17	0.10	0.19	0.17	0.53	0.35

Results

Morphological measurement

Inter-group comparison showed that the transverse distances from the median plane to Tb in the Norm and Mal groups (both the shifted and non-shifted sides) were significantly shorter than those in the control group ($p < 0.05$) (Tables 2 and 3). The transverse distances from the median plane to Oc in the Norm and non-shifted sides in the Mal group were significantly shorter than those in the control group ($p < 0.01$). The transverse distance from the median plane to S1 on the non-shifted side in the Mal group was significantly shorter than that in the control group ($p < 0.05$). On the other hand, almost all a-p distances in the Norm and Mal groups were significantly shorter than those in the control group ($p < 0.05$). The a-p distances of SC-A, SC-Pr, N-Pr, and N-A in the Mal group were significantly shorter than those in the Norm group ($p < 0.05$). The transverse deviations from the median plane to Pr and A in the Mal group were significantly larger than those in the control and Norm groups ($p < 0.05$).

In the Mal group, intra-group comparison showed that there were no significant differences between the shifted and non-shifted sides in all transverse distances (Tables 2 and 3).

Table 3. ***p*** **Values of one-way analysis of variance among control (1), Norm (2) and Mal [shifted (3) and non-shifted (4) sides] groups. Upper, transverse distances; middle, antero-posterior (a-p) distances; lower, transverse deviations**

	p Value (transverse distances)					
	1 vs. 2	1 vs. 3	1 vs. 4	2 vs. 3	2 vs. 4	3 vs. 4
Oc	0.003	0.000	0.146	0.755	0.414	0.069
Tb	0.001	0.000	0.018	0.972	0.757	0.495
S2	0.908	0.528	0.781	0.194	0.993	0.115
S1	0.345	0.026	0.844	0.584	0.822	0.159

	p Value (a-p distances)		
	1 vs. 2	1 vs. 3	2 vs. 3
Ba-SC	0.008	0.003	0.922
Ba-N	0.000	0.000	0.323
Ba-Pr	0.000	0.000	0.369
Ba-A	0.000	0.000	0.094
SC-N	0.001	0.000	0.221
SC-A	0.000	0.000	0.012
SC-Pr	0.000	0.000	0.017
N-Pr	0.001	0.000	0.018
N-A	0.000	0.000	0.010
Pr-A	0.383	0.010	0.177

	p Value (transverse deviations)		
	1 vs. 2	1 vs. 3	2 vs. 3
Ba	0.409	0.797	0.914
SC	0.491	0.977	0.276
Pr	0.919	0.003	0.019
A	0.998	0.022	0.034

Mirroring image

Superimposition in the Mal group at both ages showed that the mirroring image corresponded with the original image in the central and posterior regions and that the mirroring image was completely different from the original image in the anterior region (Fig. 2).

Discussion

In the posterior cranial and maxillary region (behind S2) such as the occipital bone and the tympanic bulla, the cranial and maxillary width in *bm/bm* mice was significantly smaller than that in control mice. It was thought that transverse growth in the posterior cranial and maxillary region mainly consisted of sutural and periosteal growth (22). Thus, it was speculated that disturbance of cartilage associated with the *bm* gene might also affect sutural and periosteal growth.

It was histologically shown that undersulphated GAGs cause a disturbance of endochondral growth at the cranial base with synchondrodial joints in *bm/bm* mice (5). In this study, 3D-CT images showed that the cranial base of *bm/bm* mice was significantly smaller than that of control mice. It was also shown that the nasal septum of *bm/bm* mice was significantly shorter than that of control mice. Some studies have shown that the cranial base (the spheno-occipital synchondrosis) is a representative growth site for the craniofacial structures (23, 24) and that cartilage of the nasal septum may play an important role as a

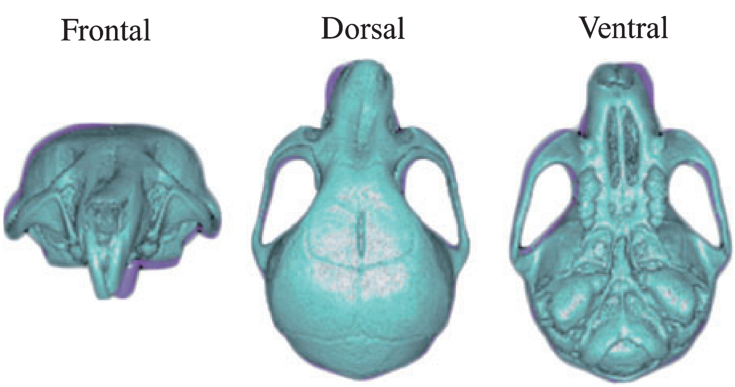

Fig. 2. Superimposition of the median plane in the Mal group (*bm/bm* mouse). Left, frontal view; center, dorsal view; right, ventral view. The central and posterior regions were almost symmetric, but the anterior region was asymmetric.

pacemaker of maxillary growth in total growth (25–29). Additionally, it was shown that disorders affecting endochondral ossification in the nasal septal cartilage may contribute to the hypo-growth of anterior craniofacial structures of *bm/bm* mouse (30). It was suggested that endochondral ossification such as that in the cranial base and nasal septum might be disturbed, which may induce a disturbance of antero-posterior growth at the cranial base and nasal septum in the *bm/bm* mouse.

The nasal septum of *bm/bm* mice with malocclusion was significantly shorter than that of *bm/bm* mice without malocclusion. The shortened nasal septum might be associated with the transverse deformity of the alveolar process of maxilla and nasal bone of the *bm/bm* mouse with malocclusion.

In *bm/bm* mice with malocclusion (transverse crossbite), the transverse deviations from the median plane to Pr and A (anterior region) were significantly larger than those in control mice and *bm/bm* mice without malocclusion, although there were no significant differences among the three groups in transverse deviations from the median plane to SC and Ba (central and posterior regions). The reason that the mean value in the transverse deviations was very small is that the points (Ba, SC, Pr, and A) were almost adjacent to the median plane. Mirroring image also showed the same results. Original and mirroring images at the central and posterior regions were nearly symmetric, but those at the anterior region showed asymmetry. Thus, it was shown that the alveolar process of maxilla and nasal bone was significantly bent in *bm/bm* mice with spontaneous malocclusion.

Conclusions

The following conclusions were obtained from 3D micro-CT images.

(1) The transverse width of the posterior cranial and maxillary complex of *bm/bm* mice was smaller than that of control mice.
(2) The cranial base and the nasal septum of *bm/bm* mice were significantly shorter than those of control mice.
(3) The nasal septum of *bm/bm* mouse with malocclusion (transverse crossbite) was significantly shorter than that of *bm/bm* mice without malocclusion.
(4) The *bm/bm* mice with spontaneous malocclusion showed a significant lateral deviation of the maxilla and nasal bone.

Clinical relevance

In this study, malocclusion and deformity at the cranium and maxilla of an animal model were evaluated using three-dimensional images (micro-CT). Presently, the maxillofacial morphology of humans is still evaluated using two-dimensional cephalometric analysis for orthodontic diagnosis. From this study, however, it is suggested that three-dimensional estimation using CT should be applied for orthodontic diagnosis of patients with maxillofacial deformities.

Acknowledgements: This research was supported by Ministry of Education, Culture, Sports, Science and Technology (17659644 to J.I., 18791541, 22792031 to Y.S-K.).

References

1. Hirabayashi Y, Fujimori O, Shimizu S. Bruch's membrane of the brachymorphic mouse. *Med Electron Microsc* 2003;36:139–46.
2. O'Brien EP, Novak EK, Keller SA, Poirier C, Guenet JL, Swank RT. Molecular map of chromosome 19 including three genes affecting bleeding time: *ep*, *ru*, and *bm*. *Mamm Genome* 1994;5:356–60.
3. Rusiniak ME, O'Brien EP, Novak EK, Barone SM, McGarry MP, Reddington M et al. Molecular markers near the mouse brachymorphic (*bm*) gene, which affects connective tissues and bleeding time. *Mamm Genome* 1996;7:98–102.
4. Tsukamoto Y, Kajii TS, Oonishi Y, Sugawara-Kato Y, Hirabayashi Y, Iida J. Histological and histochemical study of the spheno-occipital synchondrosis of the cranial base on BALB/c-*bm/bm* mouse. *Orthodontic Waves* 2006;65:166–72.
5. Tsukamoto Y, Kajii TS, Oonishi Y, Sugawara-Kato Y, Hirabayashi Y, Iida J. Growth and development of the cranial base in mice that spontaneously develop anterior transverse crossbite. *Am J Orthod Dentofacial Orthop* 2008;134:676–83.
6. Schwartz NB, Lyle S, Ozeran JD, Li H, Deyrup A, Ng K et al. Sulfate activation and transport in mammals: system components and mechanisms. *Chem Biol Interact* 1998;109:143–51.
7. Schwartz NB, Ostrowski V, Brown KS, Pratt RM. Defective PAPS-synthesis in epiphyseal cartilage from brachymorphic mice. *Biochem Biophys Res Commun* 1978;82:173–8.
8. Kurima K, Warman LM, Krishnan S, Domowics M, Krueger RC Jr, Deyrup A et al. A member of a family of sulfate-activating enzymes causes murine brachymor-

phism. *Proc Natl Acad Sci USA* 1998;95:8681–5.
9. Stelzer C, Brimmer A, Hermanns P, Zabel B, Dietz UH. Expression profile of Papss2 (3′-phosphoadenosine 5′-phosphosulfate synthase 2) during cartilage formation and skeletal development in the mouse embryo. *Dev Dyn* 2007;236:1313–8.
10. Kajii TS, Hirabayashi Y, Fujimori O, Tsukamoto Y, Oonishi Y, Sugawara-Kato Y et al. Histological and biochemical evaluation of temporomandibular joints of BALB/c-*bm/bm* mouse that spontaneously induces anterior transverse crossbite. *Dent Jpn* 2006;42:187–90.
11. Tsukamoto Y, Kajii TS, Sugawara-Kato Y, Hirabayashi Y, Fujimori O, Iida J. Relationship between degree of malocclusion and occlusal interference in mice that spontaneously develop anterior transverse crossbite. *Am J Orthod Dentofacial Orthop* 2010;138:710.e1–5.
12. Papadopoulos MA, Jannowitz C, Boettcher P, Henke J, Stolla R, Zeilhofer H et al. Three-dimensional fetal cephalometry: an evaluation of the reliability of cephalometric measurements based on three-dimensional CT reconstructions and on dry skulls of sheep fetuses. *J Craniomaxillofac Surg* 2005;33:229–37.
13. Pelo S, Tessiello S, Boniello R, Gasparini G, Longobardi G. A new method for assessment of craniofacial malformations. *J Craniofac Surg* 2006;17:1035–9.
14. Muramatsu A, Nawa H, Kimura M, Yoshida K, Maeda M, Katsumata A et al. Reproducibility of maxillofacial anatomic landmarks on 3-dimensional computed tomographic images determined with the 95% confidence ellipse method. *Angle Orthod* 2008;78:396–402.
15. Ishii T, Yamaguchi H. Influence of extraoral lateral force loading on the mandible in the mandibular development of growing rats. *Am J Orthod Dentofacial Orthop* 2008;134:782–91.
16. Hallgrímsson B, Brown JJ, Ford-Hutchinson AF, Sheets HD, Zelditch ML, Jirik FR. The brachymorph mouse and the developmental-genetic basis for canalization and morphological integration. *Evol Dev* 2006;8:61–73.
17. Wang Y, Sun M, Uhlhorn VL, Zhou X, Peter I, Martinez-Abadias N et al. Activation of p38 MAPK pathway in the skull abnormalities of Apert syndrome Fgfr2(+P253R) mice. *BMC Dev Biol* 2010;10:22.
18. Twigg SR, Healy C, Babbs C, Sharpe JA, Wood WG, Sharpe PT et al. Skeletal analysis of the Fgfr3(P244R) mouse, a genetic model for the Muenke craniosynostosis syndrome. *Dev Dyn* 2009;238:331–42.
19. Hachiya N, Ohtaishi N. *Methods of Preparing Osteal Specimens*. Sapporo: Hokkaido University Press; 1994.
20. Min S, Sato S, Saito M, Ebihara H, Arai Y, Ito K. Micro-computerized tomography analysis: dynamics of bone augmentation within a titanium cap in rabbit calvarium. *Oral Surg Oral Med Oral Pathol Oral Radiol Endod* 2008;106:892–5.
21. Martin R, Knussmanb R. *Anthropologie, Handbuch der vergleichenden Biologie de Menschen*. Stuttgart: Gustav Fischer; 1988.
22. Sinclair D, Dangerfield P. *Human Growth After Birth*. Oxford: Oxford University Press; 1985.
23. Enlow DH, Moyers RE, Hunter WS, McNamara JA Jr. A procedure for the analysis of intrinsic facial form and growth. An equivalent-balance concept. *Am J Orthod* 1969;56:6–23.
24. Mizoguchi I. Study on effects of destruction of the spheno-occipital synchondrosis to the growth of the mandibular condyle in the growing rats. *J Jpn Orthod Soc* 1987;46:316–33.
25. Sicher H. Some principles of bone pathology. *J Oral Surg (Chic)* 1949;7:104–17.
26. Scott JH. The growth of the human face. *Proc R Soc Med* 1954;47:91–100.
27. Scott JH. The growth of the nasal cavities. *Acta Otolaryngol* 1959;50:215–24.
28. Latham RA. Maxillary development and growth: the septo-premaxillary ligament. *J Anat* 1969;104:584–6.
29. Sarnat BG, Wexler MR. Postnatal growth of the nose and face after resection of septal cartilage in the rabbit. *Oral Surg Oral Med Oral Pathol* 1986;26:712–27.
30. Takahashi K, Kajii TS, Tsukamoto Y, Saito F, Wada S, Sugawara-Kato Y et al. Histological study of the nasal septal cartilage in BALB/c-*bm/bm* mouse which spontaneously induces malocclusion. *Hokkaido J Dent Sci* 2011. In press.